

Quasi-Elastic Barrier Distribution for the ${}^7\text{Li} + {}^{144}\text{Sm}$ weakly bound system

Denilson R. Otomar*, Jesus Lubián, and Paulo Roberto Silveira Gomes †

Fluminense Federal University

acaqua@if.uff.br

lubian@if.uff.br

paulogom@if.uff.br

Excitation function of quasielastic scattering for the ${}^7\text{Li} + {}^{144}\text{Sm}$ system have been measured at backward angles for a range of energies from well below to above the Coulomb barrier. Furthermore, the corresponding barrier distribution was extracted by employing a numerical method which consists in the first derivate with respect to the energy of the quasielastic excitation function. The theoretical calculation was done by the CCBA formalism in the CDCC framework. The channels employed in analyzing the nuclear reaction were the *one neutron stripping* and *sequential breakup*.

XXXIV edition of the Brazilian Workshop on Nuclear Physics,

5-10 June 2011

Foz de Iguacu, Parana state, Brasil

*Speaker.

†Faperj, CAPES, CNPq and Uff

1. Introduction

In a previous work[1], we considered the role of the inelastic channels both ${}^7\text{Li}$ and ${}^{144}\text{Sm}$ in the quasielastic scattering. Beside, we computed the influence of the ${}^7\text{Li}$ breakup. Now, we perform a complete calculation for that system by including the *one-neutron stripping* channel and the *sequential breakup* channel. In the case of *one-neutron stripping* channel, its inclusion in the CDCC formalism was performed by CRC calculations. The *sequential breakup* channel consists in one-neutron stripping followed by ${}^6\text{Li}$ breakup which is assumed to split into alpha and deuterium particles[2]. The procedure to describe the data was performed within the CDCC formalism considering a cluster folding for the structure of ${}^{6,7}\text{Li}$. As the *sequential breakup* channel represents a two-step process, it was not possible to include it directly into the full CDCC calculation. So, the tricky employed was the CCBA framework, i.e., CC in the entrance channel, CDCC in the exit one and DWBA for the transfer step. All these calculations were done using the code FRESKO, and the São Paulo potential as a parameter free bare potential which explains the elastic scattering data. It is important to emphasize that no parameter search was performed to fit the data, but rather a comparison between excitation function and its barrier distribution with theoretical predictions. The quasielastic scattering is defined as

$$\sigma^{qel} = \sigma^{el} + \sigma^{inel} + \sigma^{tr}$$

It has an important application because it represents an alternative way to describe the fusion. The fusion is connected with transmission coefficient (T) through a barrier and the large angle quasielastic scattering is connected by reflection coefficient (R) through that barrier. Because the conservation of reaction flux, these two processes may be considered as complementary to each other. So, due to this complementarity, we have

$$D^{fus}(E) = -\frac{d}{dE} \left[\frac{d\sigma^{qel}(E)}{d\sigma^{Ruth}(E)} \right],$$

where the term between the brackets on the right side is the reflection coefficient (R(E)). As the breakup channel feeds states in the continuum, its role in the elastic and inelastic scattering and fusion cross section for weakly bound systems is very different from that involving tightly projectiles. Thus, for the defined quasielastic scattering, we must add breakup cross section (σ^{NCBU}). The breakup formalism is very complex, since after the fragmentation of projectile, different processes can take place. If we assume a fragmentation into two fragments, we have the following possibilities: NCBU (Non-capture breakup), the two fragments fly away; SCF (Sequential complete fusion), the two fragments are captured by the target, consecutively; ICF (Incomplete fusion), only one of the fragments is captured by the target. Therefore, for the systems involving weakly bound projectiles quasielastic scattering (NCBU) is complementary to the CF (SCF + ICF). From the experimental point of view, measuring the fusion is quite difficult because the evaporation residues have too low energy to be detected by conventional detectors window and, besides, they do not decay neither by alpha-emission nor by fission, which could be easier detected. By other hand, quasi-elastic measurement requires only the use of telescope at backward angles and counting everything impinging on it (el + inel + tr + NCBU). This is another advantage upon fusion.

2. Experimental setup

The experiments were performed at the Tandem laboratory. The detection system consisted of two ΔE -E telescopes, with thicknesses of 15 and 30 μm , respectively, and with 150 mm^2 of area. For more experimental details, see reference [1]. In Figure 1, we have a typical tri-dimensional spectrum. According to the Figure, the events associated for $Z = 1$, $Z = 2$ and $Z = 3$ can be seen and

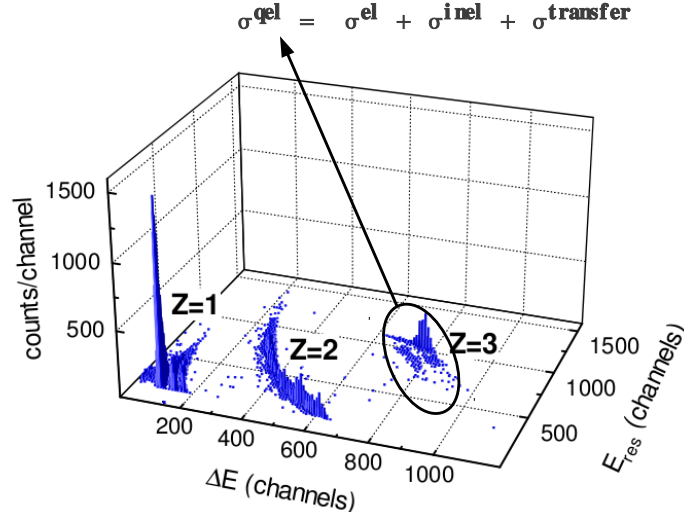


Figure 1: The tri-dimensional spectrum. The data was measured at $E_{Lab}(MeV) = 27MeV$ and $\theta_{Lab} = -155^\circ$

separated. Furthermore, for $Z = 1$, we can distinguish events associated with hydrogen, deuterium and tritium particles. For the $Z = 1$ and $Z = 2$ events were not considered in our present analysis because it was not possible to clearly distinguish the corresponding reaction channels, whether is a NCBU or transfer or evaporation of the CF an ICF (deuterium, tritium, alpha, etc.) of compound nuclei. So, $Z = 3$ events do not correspond to the full quasi-elastic cross section, but rather a lower limit of it. Then, the contributions associated with NCBU and ICF are not taken into account.

3. Theoretical formalism

3.1 Coupled Reaction Channel

To include the one-neutron transfer channel, finite range approximation, post-interaction, and full real remnant have been adopted. As the Q-value is about -0.493 MeV, only transfer to the ground state of ^{145}Sm was considered. For more details, see reference [1]. Below, we have the following coupled reaction equations (CRC)

$$[(E - \varepsilon_\alpha) - K_\alpha - \langle \alpha | V_\alpha | \alpha \rangle] u_\alpha(\vec{r}_\alpha) = \int dr_\beta K_{\alpha\beta}(\vec{r}_\alpha, \vec{r}_\beta) u_\beta(\vec{r}_\beta)$$

$$[(E - \varepsilon_\beta) - K_\beta - \langle \beta | V_\beta | \beta \rangle] u_\beta(\vec{r}_\beta) = \int dr_\alpha K_{\beta\alpha}(\vec{r}_\beta, \vec{r}_\alpha) u_\alpha(\vec{r}_\alpha),$$

where:

$$V_\alpha = V_\alpha(\vec{r}_\alpha, \vec{r}, \xi_\alpha) = V_{\alpha\text{-target}}(\vec{r}_\alpha, \vec{r}, \xi_\alpha) + V_{t\text{-target}}(\vec{r}_\alpha, \vec{r}, \xi_\alpha)$$

The kernels K include differential operators, namely the operators contained in the Hamiltonian for the kinetic energy of relative motion. For the real parts of the ${}^4\text{He} + {}^{144}\text{Sm}$ and $t + {}^{144}\text{Sm}$ optical potentials, a double-folding potential was used. For the matter densities of the ${}^{144}\text{Sm}$ target, those of the systematic of the of the São Paulo potential were used. Under these assumption that the matter density and the charge density have similar distributions, we have calculated the matter distribution of the t cluster as the sum of the charge distributions of t and ${}^3\text{He}$, which were obtained using the parameters of Ref.[4]. A similar procedure was applied for ${}^4\text{He}$, for which the matter distribution was calculated as twice its charge distribution. For the imaginary part, we use the so-called "IWBC, Ingoing Wave Boundary Conditions".

3.2 CCBA formalism

For the sequential breakup (transfer-breakup)[3], we use the formalism of CCBA which scheme can be seen in the Figure 2.

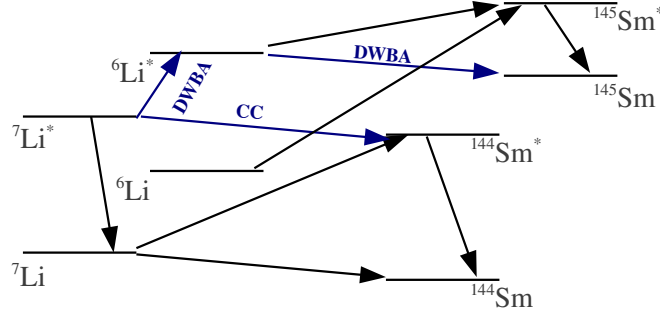


Figure 2: CCBA scheme.

In this way, the corresponding coupled equations are

$$[(E - \varepsilon_\alpha) - K_\alpha - \langle \alpha | V_\alpha | \alpha \rangle] u_\alpha(\vec{r}_\alpha) \approx 0$$

$$[(E - \varepsilon_\beta) - K_\beta - \langle \beta | V_\beta | \beta \rangle] u_\beta(\vec{r}_\beta) \approx \int dr_\alpha K_{\beta\alpha}(\vec{r}_\beta, \vec{r}_\alpha) u_\alpha(\vec{r}_\alpha),$$

where:

$$V_\beta = V_\beta(\vec{r}_\beta, \vec{r}, \xi_\beta) = V_{\alpha\text{-target}}(\vec{r}_\beta, \vec{r}, \xi_\beta) + V_{d\text{-target}}(\vec{r}_\beta, \vec{r}, \xi_\beta)$$

The diagonal potential used in the optical model (One-channel) calculations was obtained by single folding the interactions (Coulomb plus nuclear) ${}^4\text{He} + {}^{144}\text{Sm}$ and $d + {}^{144}\text{Sm}$ in the α -deuteron ground-state wave function. For the ${}^4\text{He}$, $d + {}^{144}\text{Sm}$ optical potentials, a double-folding São Paulo potential (SPP) was used. The matter density of the ${}^{144}\text{Sm}$ target was taken from the systematic of the São Paulo potential. Assuming that charge and matter densities have similar distributions, the matter density distribution of the d (deuteron) was obtained multiplying by 2 the charge distribution reported in ref.[5]. For the matter density of the ${}^4\text{He}$ cluster the same procedure was applied. In this situation, we use the São Paulo potential both the real part and the imaginary part of the potential. This is necessary, because of the presence of high-order terms. The model space used to discretization is given in Figure 3.

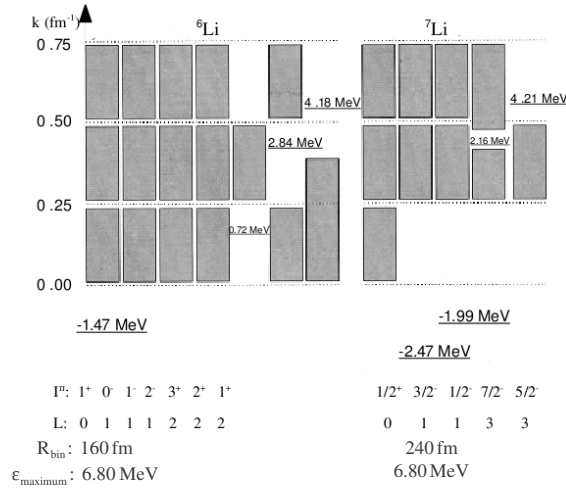


Figure 3: Model space for ${}^6,7\text{Li}$ [6, 7]

4. Results

In Fig. 4, we have a comparison between the calculus with data.

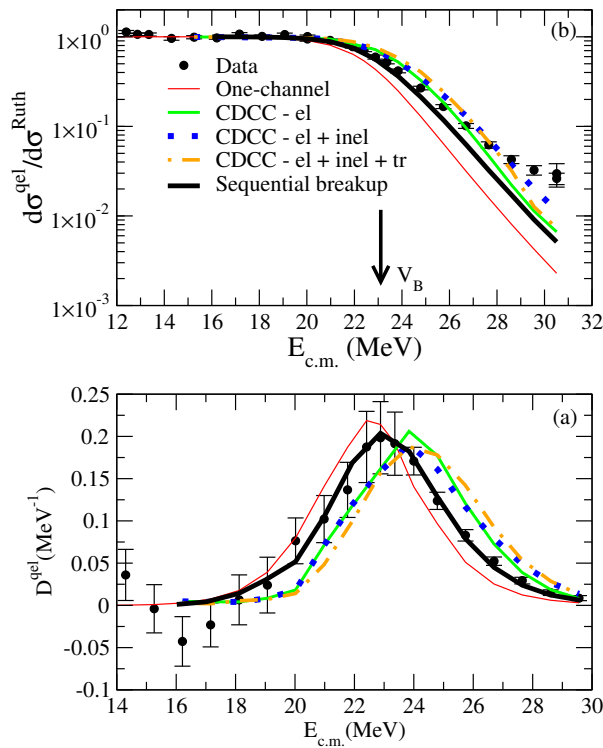


Figure 4: (a) Corresponding barrier distribution for the (a) Partial quasi-elastic excitation function at $\theta_{\text{Lab}} = 155^\circ$. The thickest line represents the CCBA calculation and the dotted-dash line represents CRC.

5. Conclusions

In conclusion, the one-neutron stripping is negligible for both the excitation function and the

corresponding barrier distribution. In the case of sequential breakup, the comparison between the excitation function with data is reasonable. For the barrier distribution the agreement is excellent, because this quantity describes well near-barrier excitation functions. The not so good agreement with the excitation function at high energies might be explained by the omission, in our calculations, of other possible transfer channels preceding the breakup, such as the pick-up of one proton[8]. The inclusion of this channel in the calculations, nevertheless, it is not easy, since it produces ${}^8\text{Be}$ that later decay into $\alpha + \alpha$.

The potential used in the sequential breakup is quite different from that used in CRC, because the presence of the second-order term in the DWBA expansion (a two-step process).

6. Acknowledgments

We would like to thank the financial support from the FAPERJ, CAPES, CNPq and the Fluminense Federal University.

References

- [1] D. R. Otomar *et al.*, Phys. Rev. C **80**, 034614 (2009).
- [2] D. H. Luong *et al.*, Phys. Lett. B **695**, (2011) 105.
- [3] A. Shrivastava *et al.* Phys. Lett. B **633** (2006) 463-468.
- [4] H. Devries, C. W. DeJager, and C. Devries, At. Data Nucl. Data Tables **36**, 495 (1987).
- [5] D. Abbott *et al.*, Eur. Phys. J. A **7**, 421 (2000).
- [6] G. R. Keeley *et al.*, Phys. Rev. C **63**, 024601 (2000).
- [7] A. Días Torres, I. J. Thompson, C. Beck, Phys. Rev. C **88**, 044607 (2003).
- [8] D. H. Luong *et al.*, Phys. Lett. **B** 695, (2011) 105.